



Synthesis and properties of perylenetetracarboxylic diimide dimers linked at the bay position with conjugated chain of different length

Yan Shi, Haixia Wu, Lin Xue, Xiyou Li*

Key Lab of Colloid and Interface Chemistry, Ministry of Education of China, Department of Chemistry, Shandong University, Jinan 250100, China

ARTICLE INFO

Article history:

Received 2 July 2011

Accepted 16 September 2011

Available online 24 September 2011

Keywords:

Perylenetetracarboxylic diimide

Dimer

Aggregation

Fluorescence spectrum

Absorption spectrum

ABSTRACT

Three perylenetetracarboxylic diimide (PDI) dimers linked with a conjugated chain of different lengths have been designed and prepared. The UV–Vis absorption and fluorescence spectra of these three dimers revealed different photophysical properties owing to the different length of the linkage. The intermolecular π – π interactions were found to be enhanced significantly with the increase in the length of the linkage and therefore induced different aggregation behaviors of these molecules. The structure of the molecular aggregates was investigated by X-ray diffraction (XRD), and the morphology of the aggregates was examined by atomic force microscopy (AFM). One-dimensional fibers were observed for the aggregates of compounds **2** and **3**, and thin solid films were observed for the aggregates of compound **1**.

© 2011 Elsevier Inc. All rights reserved.

1. Introduction

Perylenetetracarboxylic diimides (PDIs) are currently being investigated for use as a variety of photoactive organic materials because of their excellent thermal and light stability, high luminescence efficiency and variable optoelectronic properties [1–3]. They were widely studied as n-type semiconductors in field-effect transistors, chromophores as light-harvesting components in solar cells, and robust organic dyes that are resistant to photobleaching [4–13]. Because of the strong π – π interactions between the planar PDI rings, they are also good building blocks for self-organized molecular materials with highly ordered structure [14–34].

A recently developed strategy for the design and synthesis of self-organized organic material is connecting several planar conjugated organic molecules into one macromolecule. The π – π interactions between neighboring molecules can be reinforced significantly in this system and, therefore, can drive the molecules self-assemble into molecular aggregates with not only highly ordered structure but also large dimensional size [35]. A porphyrin ring covalently connected with four PDI units has been prepared by Wasielewski and co-workers [11]. The coplanar conformation of these PDI units has reinforced the π – π interactions between the molecules and induces the formation of large aggregates in solution with high stability. Similarly, a phthalocyanine appended with four PDI units at peripheral positions can form a heptamer in nonpolar solvents with a well-defined face-to-face stacked structure [36]. More interestingly, quick and efficient energy transfer

between the aggregated PDIs and phthalocyanines was observed. Three PDI units connected by a rigid 1,3,5-triphenyl benzene group formed a propeller-like PDI trimer [37]. This PDI trimer self-aggregated into one-dimensional nanofibers with very large aspect ratios. In a similar trimer, electron donors, *N,N*-diethylaniline, were introduced at one end of the PDI molecules [38]. The resulted compound exhibits non-covalent dimerization in solution and leads to a variety of changes on its photophysical properties in comparison with the monomers. We have prepared a series of PDI trimers with triazine ring as the linkage [39]. The branched structure together with the coplanar conformation leads to the reinforced π – π interactions between the molecules and thus improves the structure order of the nano-self-assembly. A hexaazatriphenylene linked with six PDI units self-assemble in both solution and solid films to form a highly stabilized dimeric aggregate in which energy transfer from the hexaazatriphenylene core to the PDI moieties occurs efficiently [40]. All the work mentioned above have clearly revealed that connection of several planar PDI rings in one molecule is an efficient way to reinforce the aggregation of organic molecules. However, all the PDI oligomers mentioned above are connected at imide nitrogen atoms. PDI oligomers linked at bay positions are still scarcely reported in literature [41,42].

Controllable self-assembling of small organic molecules into organic nano-material is the most attractive field of molecular electronics. “Controllable” here means not only the controllable structure of the self-assembly but also predictable inter- or intramolecular interactions of the molecules, which cause novel properties for the material. Therefore, programming the inter- and/or intramolecular interactions during the molecular design is extremely important to achieve a novel organic self-assemble material. In the present

* Corresponding author. Fax: +86 531 8856 4464.

E-mail address: xiyouli@sdu.edu.cn (X. Li).

work, we designed three PDI dimers (Scheme 1), which linked with conjugated chain at the bay positions. The rigid conjugated linkage between the two PDI units renders a rigid conformation for the whole molecule, and therefore, less conformation change occurs during the self-assemble process. This will be helpful to keep the properties of single molecule in the molecular self-assembly. Moreover, the conjugated chain between the PDI units can enhance the interactions between the aromatic systems of the linked two PDI units, which might induce significant change on the photophysical properties of PDIs in relative to their monomeric form. To the best of our knowledge, this represents the first example of the molecular self-assembly of PDI dimers linked with rigid conjugated chain.

2. Materials and methods

2.1. General methods

Electronic absorption spectra were recorded on a Hitachi 4100 spectrometer. Fluorescence spectra were measured on an ISS K2 system. MALDI-TOF mass spectra were taken on a Bruker BIFLEX III mass spectrometer with α -cyano-4-hydroxycinnamic acid as the matrix. The low-angle X-ray diffraction (LAXD) experiment was carried out on a Rigaku D/max- γ B X-ray diffractometer. The morphology of nanostructures was measured in air by using a Veeco multimode atomic force microscope (AFM) in tapping mode. The minimized molecular structure was calculated at DFT/B3LYP/6-31 g(d) level.

2.2. Materials and methods

All solvents were of analytical grade and purified using standard methods [43]. 1,7-Di(*p*-*t*-butyl-phenoxy)-3,4,9,10-tetracarboxylic dianhydride [27] and monomers **4**, **5** and **6** were synthesized by the procedures described previously [44].

3. Results and discussion

3.1. Molecular design and synthesis

PDI dimers linked by ethynylene or butadiynylene at bay positions have been prepared by Zhao recently [41]. The absorption and emission spectra as well as the electrochemistry are reported. However, the intermolecular interactions between the PDI units of these compounds were not discussed in the literature. In order to evaluate the effect of the chain length of the conjugated spacer on the intermolecular aggregation behavior of these dimeric PDIs, we introduced longer conjugated spacers into these series of compounds. Meanwhile, long alkyl chains are introduced to the other bay positions of PDI ring which are expected to further enhance the aggregation in solvents.

The three dimers, **1**, **2** and **3**, were prepared from PDIs (**4**, **5**, **6**) with alkyne substituents at the bay position via oxidation

condensation, Scheme 1. All the reactions were carried out in DMF at 80 °C with CuI and I₂ as catalysts. The ¹H NMR spectra of **1**, **2** and **3** in deuterated chloroform display severely broadened peaks, which indicates that these three compounds form aggregates easily in chloroform. The detailed synthetic procedures are described in the Supporting information.

3.2. Electronic absorption spectra in solutions

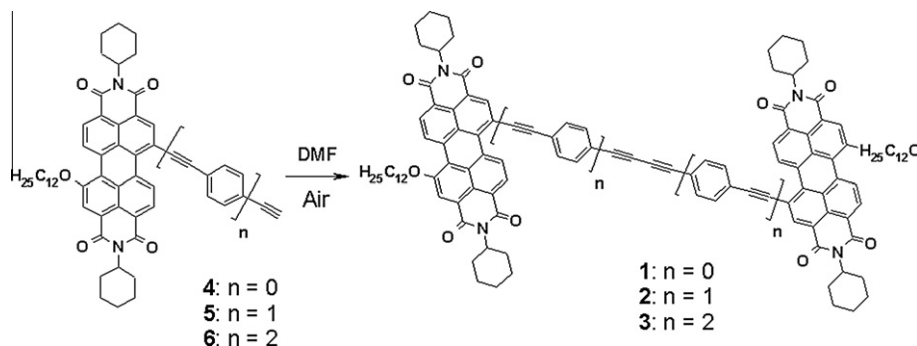
Owing to the strong π - π interactions between the PDI units of different molecules, all these dimers show very small solubility in CHCl₃. In order to get satisfactory absorption spectra, a mixed solvent of chloroform/toluene (1:1) was used in all spectroscopic measurements.

The absorption spectra of compounds **1**–**3** in the mixed solvent of chloroform and toluene are shown in Fig. 1A–C, and the spectral parameters are summarized in Table 1. For comparison purpose, the absorption spectra of monomeric PDI **4**–**6** in the same solvent are also presented in Fig. 1. Compared with that of monomeric **4**, the broad absorption band of **1** in the region of 500–650 nm experienced a significant shift to red, and the absorption band edge shifted from 600 nm for monomeric **4**–650 nm for dimeric **1**, which may be ascribed to the extension on the conjugation system in dimeric **1**. However, the maximum absorption peak of **1** blue-shifted significantly from 563 nm to 534 nm as shown in Fig. 1A, which indicates the presence of strong π - π interactions between the PDI units of **1**. Similar blue shift has been attributed to the intermolecular face-to-face stacking of PDI rings and the formation of H-type aggregates in literature [45,46]. But we found that the absorption spectra of **1** is not concentration dependent and keep the same shape even in a very diluted solution. This result suggests that the blue shift on the maximum absorption peak of **1** relative to that of **4** is not caused by an intermolecular interaction but by an intramolecular interaction instead. The significant enhancement on the absorption of **1** relative to that of monomeric **4** in the region of 350–400 nm can be attributed to the conjugated linkage.

The absorption spectra of **2** in the mixed solvent are significantly different from those of **1**, but similar with those of monomeric **5** in shape. This suggests no strong interactions between the two PDI units in the molecule of **2**, probably due to the large separation between the two PDI units. Similar to that observed in the absorption spectra of **1**, the absorption enhancement of **2** relative to that of **5** in the range of 350–420 nm can be attributed to the conjugated bridge between the two PDI units. The absorption spectra of **3** present similar properties with those of monomeric **6**, indicates that no intramolecular interactions between the PDI units in **3**, which is similar with that observed for **2**.

3.3. Fluorescence spectra

As displayed in Fig. 2, the fluorescence spectra of **1** in the mixed solvent show a significantly red-shifted emission band with very



Scheme 1. Synthesis of PDI dimers.

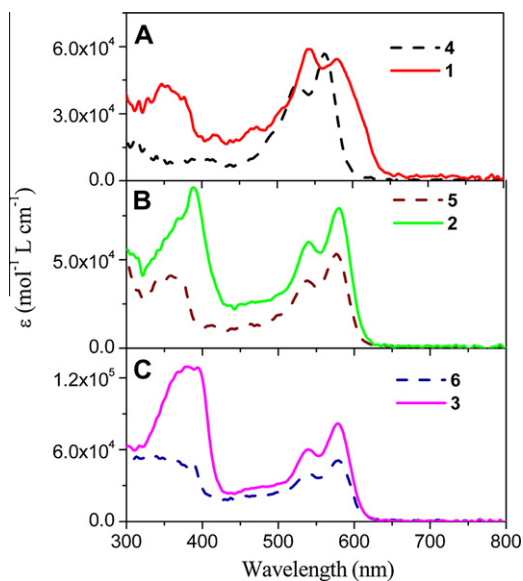


Fig. 1. The absorption spectra of **1** (A), **2** (B) and **3** (C) in the mixed solvent of chloroform/toluene (1:1) with a concentration of 1×10^{-6} mol L $^{-1}$. For comparison purpose, the absorption spectra of **4**, **5** and **6** recorded in the same concentration are also shown. (For interpretation of the references to color in this figure legend, the reader is referred to the web version of this article.)

Table 1

Comparison of the spectroscopic parameters of **1–6** at 1×10^{-6} mol L $^{-1}$ in mixed solvent.

Compounds	λ_{abs} (nm)	λ_{em} (nm)	Φ_f (%)
1	534	638	7.64
2	531	609	39.15
3	530	608	34.53
4 [44]	562	587	85.77
5 [44]	576	603	80.85
6 [44]	579	605	59.50

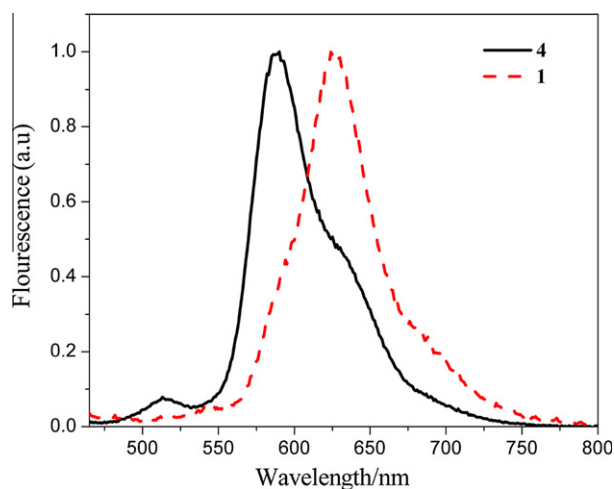


Fig. 2. Normalized fluorescence spectra of **1** and **4** in dilute solution in the mixed solvent of CHCl $_3$ /toluene (1:1) (concentration: 1×10^{-6} mol L $^{-1}$). Excitation wavelength is 450 nm. (For interpretation of the references to color in this figure legend, the reader is referred to the web version of this article.)

low fluorescence quantum yield in comparison with those of monomeric **4** (Table 1). This red-shifted emission can be attributed to the efficient intramolecular π – π interactions between the PDI units in **1** [47]. This is in accordance with the results of electronic

absorption spectra as mentioned above. However, the fluorescence spectra of **2** and **3** (Supporting information, Fig. S1) are similar with those of monomeric **5** and **6**, respectively, and no significant change on the emission wavelength as well as fluorescence quantum yield was observed. This result indicates that there is no intramolecular interaction between the PDI units of **2** or **3**, and it is in good accordance with the results of absorption spectra.

3.4. Aggregation behavior in solution

UV–Vis absorption spectra of PDIs are sensitive to the interchromophore distance and orientation and therefore have been widely used to study their π – π stacking [17,39]. Fig. 3A shows the absorption spectra of **1** in a mixed solvent of 1:1 CHCl $_3$ /toluene at different concentrations. At low concentration (5×10^{-7} mol L $^{-1}$), the spectra of **1** show two peaks at 541 and 579 nm, which correspond to the 0–0 and 0–1 transitions, respectively [33]. Following the previous report, the 0–0 and 0–1 transitions will reverse in intensity upon π – π stacking [48–50]. Therefore, the intensity ratio of the peaks at 541 and 579 nm is directly correlated with the proportion of aggregates against monomer in solution. In a much diluted solution, such as 5×10^{-7} mol L $^{-1}$, the absorption of **1** presents a spectrum with the peak intensity at 541 nm larger than that at 579 nm, which indicates the presence of strong π – π interaction between the PDI units of **1** in the diluted solution. The peak intensity ratio A_{579}/A_{541} does not change distinctly along with concentration increase in the range of 5×10^{-7} – 5×10^{-6} mol L $^{-1}$, which suggests that the interaction between the PDI units of **1** in this diluted solution is concentration independent, and therefore, the interaction between the PDI units, which caused the blue shift on the maximum absorption band, is an intramolecular process. However, in more concentrated solution, such as 1×10^{-5} – 5×10^{-5} mol L $^{-1}$, the peak intensity at 579 nm drops significantly along with concentration increase, which indicates the formation of molecular

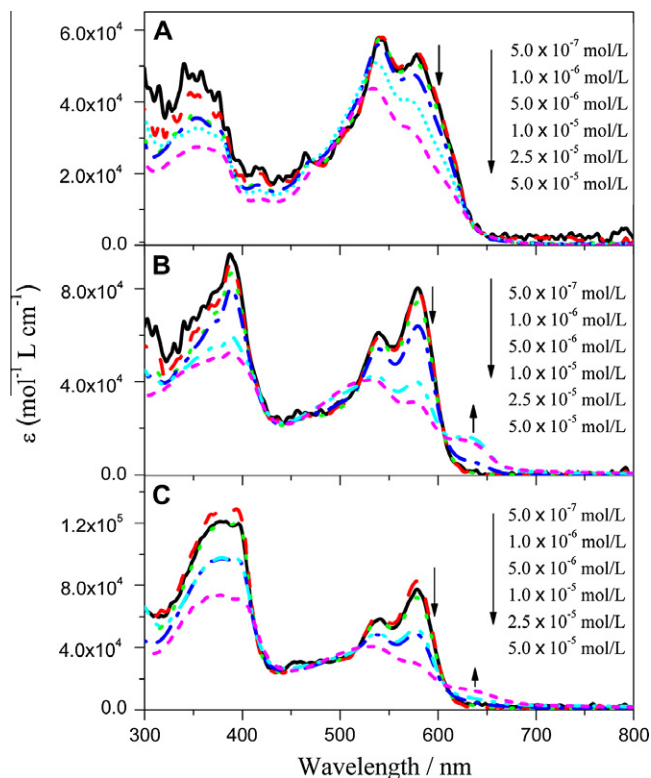


Fig. 3. Concentration-dependent absorption spectra of **1** (A), **2** (B) and **3** (C) in 1:1 CHCl $_3$ /toluene. (For interpretation of the references to color in this figure legend, the reader is referred to the web version of this article.)

aggregates at this concentration via an intermolecular self-assembly process.

The absorption spectra of **2** show the maximum absorption band at 580 nm, which is almost same with those of monomer **5**. The absorption spectra of **2** do not change along with the concentration increase in the low concentration range, 1×10^{-5} – 5×10^{-7} mol L⁻¹ (Fig. 3B), which indicates not only that no intramolecular interactions between the PDI units in **2** but also that no intermolecular aggregation happened in these diluted solutions. However, when the concentration of **2** in the mixed solvent increases from 2.5×10^{-5} to 5×10^{-5} mol L⁻¹, the absorption spectra of **2** present an intensity reverse between the absorption band at 541 nm and 579 nm; meanwhile, a small shoulder appears at about 640 nm. The changes on the absorption spectrum of **2** along with concentration increase can be attributed to the formation of co-facially arranged dimeric structure [10]. Similar to those of **2**, the absorption spectra of **3** show no changes along with the concentration increase in the range of 5×10^{-6} – 5×10^{-7} mol L⁻¹ (Fig. 3C). But when the concentration increased to 1×10^{-5} mol L⁻¹, the absorption spectra show distinctive characters of co-facially stacked PDIs as those observed for **2**.

In addition to the absorption spectra, the fluorescence spectra are also sensitive to the aggregation of PDI molecules [39]. Fig. 4 shows the fluorescence spectra of **1**, **2** and **3** in a mixed solvent of 1:1 CHCl₃/toluene at different concentrations. The fluorescence spectra of **1** show one broad band centered at about 630 nm. The wavelength of this emission band together with the fluorescence quantum yield does not change significantly in the concentration range of 5×10^{-7} – 5×10^{-6} mol L⁻¹, which indicates that **1** does not aggregate in diluted solution. However, when the concentration increased from 1×10^{-5} mol L⁻¹ to 2.5×10^{-5} mol L⁻¹, the maximum emission band shifts to red slightly and a weak emission peak at about 700 nm appears, which indicates the formation of

aggregates of **1** at this concentration. This result is in accordance with the results of absorption spectra as mentioned above.

The fluorescence spectra of **2** in diluted solution (5×10^{-7} – 1×10^{-6} mol L⁻¹) are similar with those of monomer **5**, which indicates that no molecular aggregate is formed. However, when the concentration of **2** increased to 1×10^{-5} mol L⁻¹, a new emission peak at about 660 nm is observed, which can be ascribed to the “excimer-like” state due to the formation of face-to-face stacked aggregates of **2** in the concentrated solution. The fluorescence spectra of **3** show similar changes along with its concentration increase with those observed for **2**.

Molecular aggregation always induce significant drop on the fluorescence quantum yield as reported in the literature [39]. The fluorescence quantum yields of **1**, **2** or **3** in diluted solution (5×10^{-7} mol L⁻¹) were represented as Φ_0 , whereas the fluorescence quantum yields of these three compounds at other concentrations were labeled as Φ . The changes on the fluorescence quantum yield along with concentration increase can be revealed directly by a plot of Φ/Φ_0 vs. concentration, insets of Fig. 4. It can be found that the fluorescence quantum yields of **1** drop more slowly than those of **2** and **3** along with concentration increase. Meanwhile, the drop on the fluorescence quantum yield of **3** is a little bit sharper than that of **2**, indicating that **3** forms aggregate more easily than **2** does. Based on these results, we can conclude that the aggregation ability increases following the order of $1 < 2 < 3$, i.e. long linkage between the PDI units favors the self aggregation.

3.5. Morphologies of the aggregates

Different aggregation models of dimers **1–3** are also verified by the different morphologies of the molecular aggregates [37]. Samples were prepared by casting a drop of solution onto a silicon surface. The morphology of the aggregates was examined by atomic force microscopy (AFM), and the results are shown in Fig. 5.

As shown in Fig. 5 and **1** formed well-distributed two-dimensional film without specific fine structure can be identified. **2** and **3** formed one-dimensional rod-like aggregates with the aspect ratio of the latter significantly larger than the former. This is reasonable because the spectroscopic studies have revealed that **1** cannot form molecular aggregates in a relative diluted solution, which suggests that the intermolecular interactions between the molecules of **1** are small. **2** and **3** can form stable molecular aggregates in a relative diluted solution, which indicates the presence of strong intermolecular interactions. This result can be attributed to the different molecular conformation caused by the different linkage between the two PDI units.

The minimized molecular structures of **1–3** are shown in Fig. 6. The two PDI units in **1** cannot take a co-planar conformation due to the short linkage between them. Therefore, face-to-face stacking of two molecules of **1** cannot be achieved easily due to the large steric hindrance. However, the minimized structures of both **2** and **3** present co-planar conformations of two PDI units. The face-to-face stacking of the molecules can repeat for many times in one direction and leads to the formation of large molecular aggregates with one-dimensional morphology.

3.6. X-ray diffraction patterns

The structures of the aggregates were further investigated by X-ray diffraction (XRD) techniques. The aggregates of **1** do not give any meaningful information in the XRD profile, which indicates no long range order for the molecular packing in the aggregates of **1**. This is in accordance with the observation of the morphology as shown in Fig. 5. But the diffraction pattern of **2** shows several peaks in the low-angle region as shown in Fig. 7. The diffraction peak at $2\theta = 3.58^\circ$, corresponding to a d space of 3.58 nm, can be

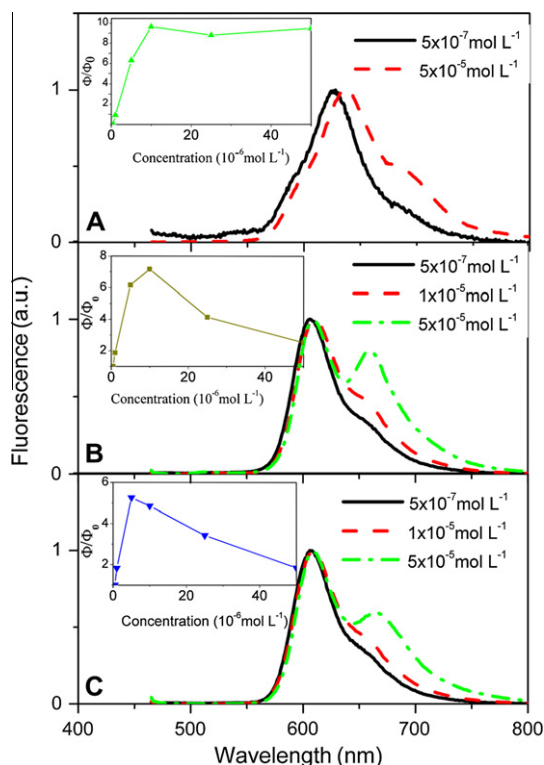


Fig. 4. Normalized fluorescence spectra of **1**, **2** and **3** (A–C) in the mixed 1:1CHCl₃/toluene solution (excitation at 450 nm). Inset show the plots of Φ/Φ_0 against the concentrations for compounds **1**, **2** and **3**. (For interpretation of the references to color in this figure legend, the reader is referred to the web version of this article.)

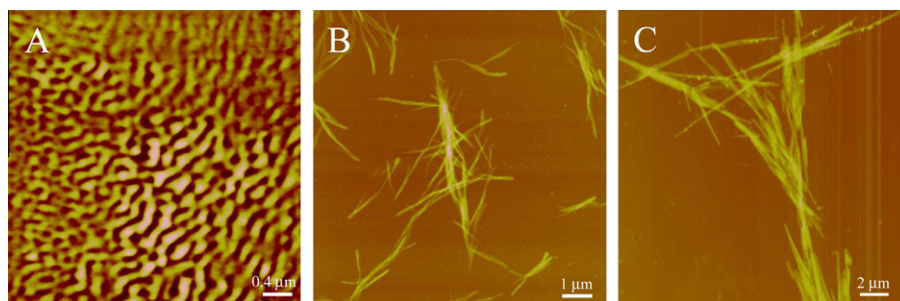


Fig. 5. AFM images of the molecular aggregates of **1**(A, $6 \mu\text{m} \times 6 \mu\text{m}$), **2**(B, $10 \mu\text{m} \times 10 \mu\text{m}$) and **3**(C, $20 \mu\text{m} \times 20 \mu\text{m}$) on silicon surface.

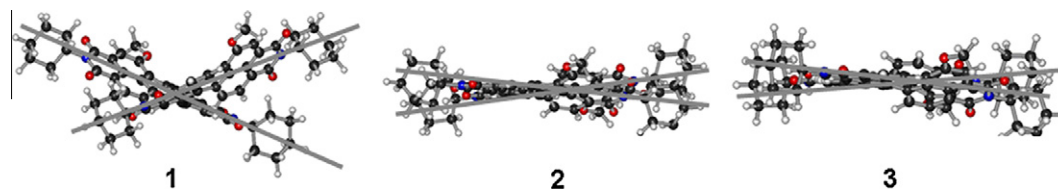


Fig. 6. The minimized molecular structures of **1–3** (alkoxy groups at bay positions were replaced with methoxy groups in calculations).

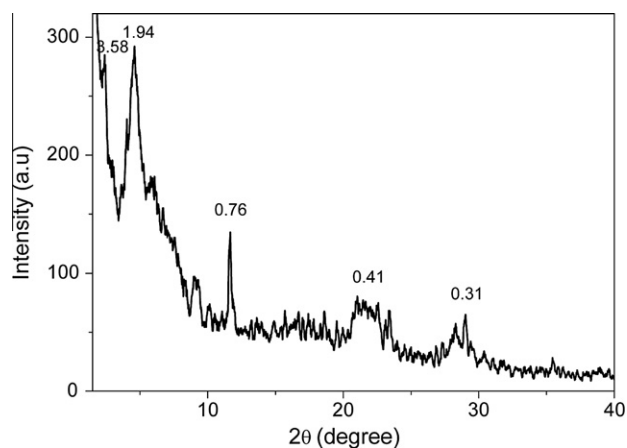


Fig. 7. XRD profile of the aggregates of dimers **2**.

ascribed to the length of the molecule. Similarly, the peak at $2\theta = 1.94^\circ$, which corresponding to a d space of 1.94 nm, can be ascribed to the width of the molecule. The sharp peak at $2\theta = 0.76^\circ$ with the d space of 0.76 nm might be attributed to the thickness of three face-to-face stacked molecules of **2** with a π - π distance of 0.38 nm. This result suggests that three stacked molecules of **2** formed a unit cell in the aggregates. Although the morphology of **3** is similar with that of **2**, the XRD profile of **3** (Supporting information) is different from that of **2**. No distinctive diffraction peaks are found, which suggests no long range order in the aggregates of **3**. This result reminds us that even though **3** formed molecular aggregates more easily than **2** as revealed by the concentration-dependent fluorescence spectra, the molecular aggregates of **3** do not have long range order on structure. Large driving force for the molecular aggregation does not necessarily lead to long range order in the molecular aggregates.

4. Conclusions

In summary, three of PDI dimers linked by ethynyl and phenyls were prepared and their molecular structures were characterized. Both experimental and theoretical studies showed that ethynyl

and phenyls are suitable linkages to extend the effective conjugation length and enhance π - π interaction. A short conjugation linkage leads to strong intramolecular interactions between the PDI units and varies the photophysical properties significantly. However, the longer linkage between the two PDI units hinders the intramolecular interactions between PDI units, but it renders a co-planar conformation for the two PDI units, and therefore, enhanced intermolecular interactions are achieved. Driven by this strong intermolecular interaction, molecules can self-assemble along one direction and form one-dimensional nano-fibers. The results of this research revealed clearly that the inter- or intramolecular interactions can be controlled by the length of the conjugated linkage. Oligomers of PDI linked with flexible non-conjugated linkages present normally properties of single PDI molecules without significant interactions between their components [39,51]. However, interactions between the PDI units in an oligomer are favored in some cases, such as the electron transfer or energy transfer in an artificial light-harvesting system. Therefore, conjugated linkages are preferred in these special occasions because it can transmit π - π interactions to a relative long distance as revealed in compound **1**. We believe that these results will be helpful in guiding the design of new organic molecules for the self-assemble organic functional materials in molecular electronic devices.

Acknowledgments

Financial support from Natural Science Foundation of China (21073112, 20871055), Natural Science foundation of Shandong Province (ZR2010EZ007) and Key lab of photochemistry of Chinese academy of science is gratefully acknowledged.

Appendix A. Supplementary material

Supplementary data associated with this article can be found, in the online version, at doi:10.1016/j.jcis.2011.09.036.

References

- [1] K.-Y. Law, Chem. Rev. 93 (1993) 449–486.
- [2] B.A. Gregg, J. Phys. Chem. B 107 (2003) 4688–4698.
- [3] R.A. Cormier, B.A. Gregg, Chem. Mater. 10 (1998) 1309–1319.
- [4] D. Gosztoła, M.P. Niemczyk, M.R. Wasielewski, J. Am. Chem. Soc. 120 (1998) 5118–5119.

- [5] Y. Zhao, M.R. Wasielewski, *Tetrahedron Lett.* 40 (1999) 7047–7050.
- [6] R.T. Hayes, M.R. Wasielewski, D. Gosztola, *J. Am. Chem. Soc.* 122 (2000) 5563–5567.
- [7] E.M. Just, M.R. Wasielewski, *Superlattice. Microstruct.* 28 (2000) 317–328.
- [8] S.E. Miller, Y. Zhao, R. Schaller, V. Mulloni, E.M. Just, R.C. Johnson, M.R. Wasielewski, *Chem. Phys.* 275 (2002) 167–183.
- [9] A.S. Lukas, Y. Zhao, S.E. Miller, M.R. Wasielewski, *J. Phys. Chem. B* 106 (2002) 1299–1306.
- [10] J.M. Giaimo, A.V. Gusev, M.R. Wasielewski, *J. Am. Chem. Soc.* 124 (2002) 8530–8531.
- [11] T. Van der Boom, R.T. Hayes, Y. Zhao, P.J. Bushard, E.A. Weiss, M.R. Wasielewski, *J. Am. Chem. Soc.* 124 (2002) 9582–9590.
- [12] M.J. Ahrena, M.J. Fuller, M.R. Wasielewski, *Chem. Mater.* 15 (2003) 2684–2686.
- [13] M. Andersson, L.E. Sinks, R.T. Hayes, Y. Zhao, M.R. Wasielewski, *Angew. Chem. Int. Ed.* 42 (2003) 3139–3143.
- [14] S.-G. Liu, G. Sui, R.A. Cormier, R.M. Leblanc, B.A. Gregg, *J. Phys. Chem. B* 106 (2002) 1307–1315.
- [15] C.W. Struijk, A.B. Sieval, J.E.J. Dakhorst, M. van Dijk, P. Kimkes, R.B.M. Koehorst, H. Donker, T.J. Schaafsma, S.J. Picken, *J. Am. Chem. Soc.* 122 (2000) 11057–11066.
- [16] W. Wang, J.J. Han, L.-Q. Wang, L.-S. Li, W.J. Shaw, A.D.Q. Li, *Nano Lett.* 3 (2003) 455–458.
- [17] W. Wang, L.-S. Li, G. Helms, H.-H. Zhou, A.D.Q. Li, *J. Am. Chem. Soc.* 125 (2003) 1120–1121.
- [18] F. Würthner, C. Thalacker, A. Sautter, W. Schärftl, W. Ibach, O. Hollricher, *Chem. Eur. J.* 6 (2000) 3871–3886.
- [19] F. Würthner, C. Thalacker, S. Diele, C. Tschierske, *Chem. Eur. J.* 7 (2001) 2245–2253.
- [20] F. Würthner, Z. Chen, F.J.M. Hoeben, P. Osswald, C.-C. You, P. Jonkheijm, J.V. Herrikhuizen, A.P.H.J. Schenning, P.P.A.M. van der Schoot, E.W. Meijer, E.H.A. Beckers, S.C.J. Meskers, R.A.J. Janssen, *J. Am. Chem. Soc.* 126 (2004) 10611–10618.
- [21] F. Würthner, *Chem. Commun.* (2004) 1564–1579.
- [22] I.K. Iverson, S.M. Casey, W. Seo, S.-W. Tam-Chang, B.A. Pindzola, *Langmuir* 18 (2002) 3510–3516.
- [23] E.E. Neuteboom, S.C.J. Meskers, E.W. Meijer, R.A. Janssen, *J. Macromol. Chem. Phys.* 205 (2004) 217–222.
- [24] M.J. Ahrens, L.E. Sinks, B. Rybtchinski, W. Liu, B.A. Jones, J.M. Giaimo, A.V. Gusev, A.J. Goshe, D.M. Tiede, M.R. Wasielewski, *J. Am. Chem. Soc.* 126 (2004) 8284–8294.
- [25] J. Hernandez, P.A.J. de Witte, E.M.H.P. van Dijk, J. Korterik, R.J.M. Nolte, A.E. Rowan, M.F. García-Parajó, N.F. van Hulst, *Angew. Chem. Int. Ed.* 43 (2004) 4045–4049.
- [26] J.J. Van Gorp, J.A.J.M. Vekemans, E.W. Meijer, *J. Am. Chem. Soc.* 124 (2002) 14759–14769.
- [27] Y. Wang, Y. Chen, R. Li, S. Wang, W. Su, P. Ma, M.R. Wasielewski, X. Li, J. Jiang, *Langmuir* 23 (2007) 5836–5842.
- [28] F. Würthner, V. Stepanenko, Z. Chen, C.R. Saha-Möller, N. Kocher, D. Stalke, *J. Org. Chem.* 69 (2004) 7933–7939.
- [29] P. Jonkheijm, N. Stutzmann, Z. Chen, D.M. de Leeuw, E.W. Meijer, A.P.H.J. Schenning, F. Würthner, *J. Am. Chem. Soc.* 128 (2006) 9535–9540.
- [30] Z. Chen, U. Baumeister, C. Tschierske, F. Würthner, *Chem. Eur. J.* 13 (2007) 450–465.
- [31] S. Yagai, T. Seki, T. Karatsu, A. Kitamura, F. Würthner, *Angew. Chem. Int. Ed.* 47 (2008) 3367–3371.
- [32] T.E. Kaiser, H. Wang, V. Stepanenko, F. Würthner, *Angew. Chem. Int. Ed.* 119 (2007) 5637–5640.
- [33] Y. Che, A. Datar, K. Balakrishnan, L. Zang, *J. Am. Chem. Soc.* 129 (2007) 7234–7235.
- [34] V. Dehm, Z. Chen, U. Baumeiste, P. Prins, L.D.A. Siebbeles, F. Würthner, *Org. Lett.* 9 (2007) 1085–1088.
- [35] M.R. Wasielewski, *J. Org. Chem.* 71 (2006) 5051–5066.
- [36] X. Li, L.E. Sinks, B. Rybtchinski, *J. Am. Chem. Soc.* 126 (2004) 10810–10811.
- [37] P. Yan, A. Chowdhury, M.W. Holman, D.M. Adams, *J. Phys. Chem. B* 109 (2005) 724–730.
- [38] B. Rybtchinski, L.E. Sinks, M.R. Wasielewski, *J. Phys. Chem. A* 108 (2004) 7497–7505.
- [39] J. Feng, B. Liang, D. Wang, H. Wu, L. Xue, X. Li, *Langmuir* 24 (2008) 11209–11215.
- [40] T. Ishi-I, K. Murakami, Y. Imai, S. Mataka, *Org. Lett.* 7 (2005) 3175–3178.
- [41] Q. Yan, D. Zhao, *Org. Lett.* 11 (15) (2009) 3426–3429.
- [42] G. Golubkov, H. Weissman, E. Shirman, G.S. Wolf, I. Pinkas, B. Rybtchinski, *Angew. Chem. Int. Ed.* 48 (2009) 926–930.
- [43] D.D. Perrin, W.L.F. Armarego, D.R. Perrin, *Purification of Laboratory Chemicals*, Pergamon, Oxford, 1980.
- [44] D. Wang, Y. Shi, C. Zhao, B. Liang, X. Li, *J. Mol. Struct.* 938 (2009) 245–253.
- [45] F. Würthner, *Chem. Commun.* (2004) 1564–1579.
- [46] D. Horn, J. Rieger, *Angew. Chem. Int. Ed.* 113 (2001) 4460–4492.
- [47] J.M. Giaimo, J.V. Lockard, L.E. Sinks, A.M. Scott, T.M. Wilson, M.R. Wasielewski, *J. Phys. Chem. A* 112 (2008) 2322–2330.
- [48] P.M. Kazmaier, R. Hoffmann, *J. Am. Chem. Soc.* 116 (1994) 9684–9691.
- [49] M.J. Ahren, L.E. Sinks, B. Rybtchinski, W. Liu, B.A. Jones, J.M. Giaimo, A.V. Gusev, A. Goshe, D.M. Tiede, M.R. Wasielewski, *J. Am. Chem. Soc.* 126 (2004) 8284–8294.
- [50] A.E. Clark, C. Qin, A.D.Q. Li, *J. Am. Chem. Soc.* 129 (2007) 7586–7595.
- [51] L. Xue, H. Wu, Y. Shi, H. Liu, Y. Chen, X. Li, *Soft Matter* 7 (2011) 6213–6221.